Letters

A Decoupled Power and Data-Parallel Transmission Method With Four-Quadrant Misalignment Tolerance for Wireless Power Transfer Systems

Xiaofei Li, Jiefeng Hu, *Senior Member, IEEE*, Yong Li, Heshou Wang, Ming Liu, and Pengqi Deng

***Abstract*—In this letter, a new power and data-parallel transmission method for wireless power transfer (WPT) systems based on a magnetically decoupled coupling structure is proposed. Unipolar coils are used for power transfer, while series-connected perpendicular bipolar coils are used for data transfer. Data transfer coils are placed in overlap with the power transfer coils at both primary side and secondary side, respectively, to form a compact structure. Especially, the side lengths of data transfer coils are intentionally designed to be smaller than the power transfer coils. Thus, in the specific four-quadrant misalignment area, the crosstalk interference between power and data transfer channels can almost be neglected, resulting in a straightforward design of data processing circuit. With the proposed coupling structure, data transfer presents a symmetrical misalignment ability. Moreover, the data transfer channel is utilized to conduct the closed-loop control of output voltage in the WPT system. Thus, in the specific four-quadrant misalignment area, stable power transfer can also be achieved. The feasibility of the proposed power and data-parallel transfer method is verified by a 122-W laboratory prototype. The system efficiency reaches 87% and data transfer rate is 19.2 kb/s. (This letter is accompanied by a video demonstrating the experimental test).**

***Index Terms*—Decoupled coupling structure, misalignment ability, output control, wireless power transfer (WPT).**

I. Introduction

OWING to the advantages of convenience and safety, wireless power transfer (WPT) is gaining global attention and recognition in various applications, such as mobile phones, household appliances, electrical vehicles (EVs), etc. [1]–[3]. For most applications, reliable data communication between primary side and secondary side is usually needed in closed-loop control to improve system performance, e.g., output-voltage feedback control, load monitoring, synchronism, and coordination between the two sides, etc. [1]. Generally, conventional wireless communication technologies such as bluetooth, Wi-Fi, and radio frequency link can be used in WPT applications for wireless data transfer, but these technologies need complicated pairing and lead to higher system cost. Recently, research works have shown that data can be transferred on existing power transfer channel. Such parallel transmission of power and data technology is more straightforward and cost effective [3].

To achieve efficient and reliable wireless data transfer in parallel to WPT, there are three main concerns [4]: 1) the interference from the added data transfer channel to power transfer; 2) the interference from the power transfer channel to data transfer; and 3) data transfer capability.

For the first concern, it is essential that the additional data transfer channel does not affect the power transfer. Yan *et al.* [5] propose a power and data-parallel transmission method based on the triangular current concept, where power is transferred by the fundamental component, while data are transferred by the third-order harmonic. Data are modulated by changing the working frequency of the inverter. Unfortunately, this would affect the resonance and, hence, the power transfer efficiency. Son and Jang [6] propose a data transfer method based on the concept of energy injection. Data are first modulated by changing the voltage of the transmitter side, and then demodulated by exploiting the characteristics of the energy flow. However, this method would deteriorate the output voltage of power transfer, and data transfer is subject to power voltage disturbances.

As to the second concern, the interference from power transfer to data transfer should be minimized to obtain a good signal-to-noise ratio (SNR) [3]. Wang *et al.* [7] propose a power and data-parallel transmission method through separate coupling channels. Data transfer almost does not affect the power flow. However, due to the cross coupling between power and data transfer channels, the crosstalk interference from power transfer to data transfer is complicated, which is not conducive for data transfer.

Manuscript received April 13, 2019; revised May 15, 2019 and May 28, 2019; accepted May 29, 2019. Date of publication June 2, 2019; date of current version September 6, 2019. This work was supported in part by The Hong Kong Polytechnic University under Grant G-YBZ4, in part by the Hong Kong Innovation and Technology Commission under Grant ITS/281/17, and in part by the Hong Kong Research Grants Council under Grant PolyU252040/17E. *(Corresponding author: Jiefeng Hu.)*

X. Li, J. Hu, H. Wang, and M. Liu are with the Department of Electrical Engineering, The Hong Kong Polytechnic University, Hong Kong (e-mail: 569411680@qq.com; jerry.hu@polyu.edu.hk; 16104772g@connect.polyu.hk; leo.m.liu@connect.po-lyu.hk).

Y. Li is with the School of Electrical Engineering, Southwest Jiaotong University, Chengdu 614200, China (e-mail: leeo1864@163.com).

P. Deng is with the School of Automation, Chongqing University, Chongqing 400032, China (e-mail: 357619947@qq.com).

This letter has supplementary downloadable material available at http://ieeexplore.ieee.org, provided by the author.

Color versions of one or more of the figures in this letter are available online at http://ieeexplore.ieee.org.

Digital Object Identifier 10.1109/TPEL.2019.2920441

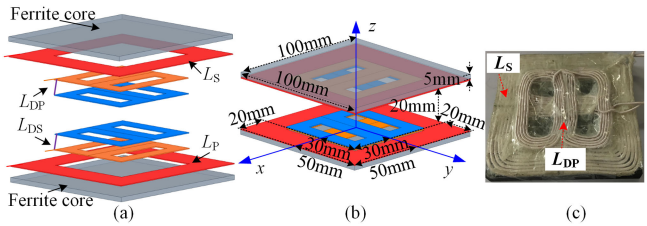

Fig. 1. (a) Proposed coupling structure. (b) Sizes of the coupling structure. (c) Manufactured coupling structure of the secondary side.

Sun *et al.* [8] propose a power and data-parallel transmission method by the same coupling channel. The proposed system has a good SNR, and the crosstalk interference between power transfer and data transfer is minimized by adding wave trappers, i.e., bandpass filter and band-reject filter. Nevertheless, in order to achieve a better filtering effect, complicated design of these wave trappers is required as they need to resonate accurately.

Last but not the least, it is desirable for data transfer with high capability, i.e., high misalignment ability. Li *et al.* [4] propose a power and data parallel transmission method, where power is transferred by inductive coils, while data are transferred by capacitive aluminum plates. The results show that data transfer has lateral misalignment tolerance. Nevertheless, when misalignment occurs, the output voltage of power transfer is significantly decreased. Another limitation is that only one direction of misalignment is considered.

To fill the aforementioned technical gap, a magnetically decoupled coupling structure is proposed here. Two unipolar coils are used to transfer power, while two series-connected perpendicular bipolar coils are used to transfer data. Data transfer coils are placed in overlap with the same-side power transfer coils, respectively, to form a compact and symmetrical structure.

The main contributions of this letter are listed as follows.

1) The side lengths of data transfer coils are intentionally designed to be smaller than power transfer coils. As a result, in the specific four-quadrant misalignment area, the crosstalk interference between power and data transfer channels can almost be neglected. Thus, compared to the methods presented in [7] and [8], the design of data transfer circuit of the proposed method is much more straightforward.
2) The utilized series-connected perpendicular bipolar coils can afford the data transfer a symmetrical misalignment ability within the specific four-quadrant misalignment area. Hence, compared to the method presented in [4], the proposed method of this letter is more reliable.

It is noted that in this letter, the parallel data transfer channel is utilized to form a closed-loop control for the power channel by delivering the WPT output voltage back to the primary side. Thus, in the specific four-quadrant misalignment area, stable power transfer can be achieved.

II. Coupling Structure

Fig. 1(a) depicts the proposed coupling structure. Two unipolar coils (L_P, L_S) with the same size are used to transfer power from the primary side to the secondary side. Two series-connected perpendicular bipolar coils (L_{DS}, L_{DP}) with the same size are used to transfer the information from the secondary side back to the primary side. To form a compact and symmetrical coupling structure, L_{DS} is placed in overlap with L_P, while L_{DP} is placed in overlap with L_S, as shown in Fig. 1(b). Ferrite cores are used on both sides to enhance the magnetic coupling. The coils are designed and manufactured completely symmetrical, as shown in Fig. 1(c). Thus, the mutual couplings between the same-side coils, i.e., the mutual coupling between L_P and L_{DS} and the mutual coupling between L_S and L_{DP}, can be neglected [9], [10]. The side length of L_{DP} and L_{DS}, i.e., $l_D = 60$ mm, is intentionally designed to be smaller than that of L_P and L_S, i.e., $l_P = 100$ mm. As a result, within the specific four-quadrant misalignment area of the secondary side, i.e., $(-(l_P - l_D)/2,\ -(l_P - l_D)/2) \le (x, y) \le ((l_P - l_D)/2,\ (l_P - l_D)/2)$, when L_S (L_P) completely covers L_{DS} (L_{DP}), the net magnetic flux generated by L_S (or L_P) will not penetrate through L_{DS} (or L_{DP}), and vice versa [11]. Therefore, the mutual inductances between power transfer coils (L_P, L_S) and data transfer coils (L_{DS}, L_{DP}) are almost zero. Consequently, the crosstalk interference between the power transfer channel and data transfer channel can be naturally suppressed.

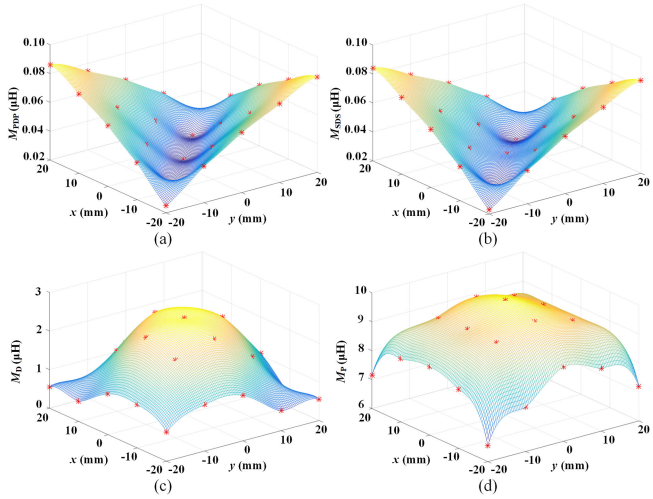

Fig. 2. Measured mutual inductances. (a) M_{PDP}. (b) M_{SDS}. (c) M_D. (d) M_P.

In this letter, 250-strand Litz wire with a diameter of 2.1 mm is used to construct the power transfer coils (L_P, L_S), and 100-strand Litz wire with a diameter of 1.35 mm is used to construct the data transfer coils (L_{DS}, L_{DP}). The number of turns of unipolar coils (L_P, L_S) and bipolar coils (L_{DS}, L_{DP}) are 11 and 10, respectively. The thickness of the ferrite core is 5 mm.

Fig. 2, which is plotted by using MATLAB, presents the measured mutual inductances, including M_{PDP} between L_P and L_{DP}, M_{SDS} between L_S and L_{DS}, M_D between L_{DP} and L_{DS}, and M_P between L_P and L_S, with different misalignments. It can be seen from Fig. 2(a) and (b) that within the specific four-quadrant misalignment area, i.e., $(-20$ mm, -20 mm$) \le (x, y) \le (20$ mm, 20 mm), the cross couplings

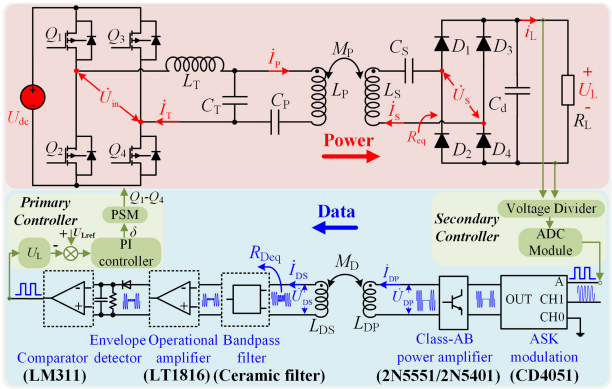

Fig. 3. Circuit diagram of the proposed WPT system.

M_{PDP} and M_{SDS} are very small and can be neglected. Therefore, the design of data transfer circuit is much more straightforward. The utilization of the series-connected perpendicular bipolar coils (L_{DS}, L_{DP}) reveals another advantage of the proposed coupling structure. That is, as can be seen from Fig. 2(c), M_D is relatively symmetrical with respect to the misalignment, thus enabling data transfer a symmetrical misalignment tolerance. The maximum (M_{DMAX}) and minimum (M_{DMIN}) of M_D are 2.49 μH and 0.52 μH, obtained at (x, y) = (0 mm, 0 mm) and (x, y) = (10 mm, -20 mm), respectively. Fig. 2(d) shows that the variation of M_P is also relatively symmetrical corresponding to the misalignment. The maximum (M_{PMAX}) and minimum (M_{PMIN}) of M_P are 9.95 μH and 6.56 μH, obtained at (x, y) = (0 mm, 0 mm) and (x, y) = (-20 mm, -20 mm), respectively.

III. Circuit Topology Analysis and System Control

A. Circuit Topology

Fig. 3 shows the circuit diagram of the proposed WPT system. The inductor–capacitor–capacitor–capacitor compensation topology is utilized in the power transfer channel, while there is no resonant compensation circuit in the data transfer channel. The output voltage of the power transfer channel is sent back to the primary side through the data transfer channel for controlling the inverter in a closed-loop manner. For simplifying the analysis, the parasitic resistances of the coils are ignored and the power semiconductors are considered to be ideal [3].

B. Analysis of the Power Transfer Channel

C_T, C_P, and C_S are the compensation capacitors with the following mathematical relation:

$$C_T = \left(\omega^2 L_T\right)^{-1}, \quad C_P = \left[{\omega_P}^2 \left(L_P - L_T\right)\right]^{-1}, \quad C_S = \left({\omega_P}^2 L_S\right)^{-1} \tag{1}$$

where ω_P is the operating angular frequency of power transfer, and it can be calculated by $2\pi f_P$ with f_P as the operating frequency of power transfer. Phase-shifted modulation is utilized to control the inverter, and the fundamental output voltage in phasor form can be expressed as

$$\dot{U}_{\text{in}} = \frac{2\sqrt{2}U_{\text{dc}}}{\pi}\sin\frac{\delta}{2}\angle 0^\circ \tag{2}$$

where δ is the conduction angle.

By using Kirchhoff's voltage law (KVL) in power transfer channel and according to the relationship between the input and output voltage of the rectifier [11], the following equations can be derived:

$$\begin{cases} \dot{U}_{\text{in}} = \left(jX_{LT} + jX_{CT}\right)\dot{I}_T - jX_{CT}\dot{I}_P \\ 0 = \left(jX_{LP} + jX_{CP} + jX_{CT}\right)\dot{I}_P - jX_{CT}\dot{I}_T - jX_{MP}\dot{I}_S \\ 0 = -jX_{MP}\dot{I}_P + \left(jX_{LS} + jX_{CS} + R_{\text{eq}}\right)\dot{I}_S \\ \dot{U}_S = R_{\text{eq}}\dot{I}_S \\ U_L = \frac{\pi\sqrt{2}}{4}U_S \end{cases} \tag{3}$$

where U_S is the root-mean-square value of $\dot{U}_{\text{S}}$ and

$$\begin{cases} X_{LT} = \omega_P L_T \; X_{CT} = 1/\omega_P C_T \; X_{LP} = \omega_P L_P \; X_{CP} \\ \qquad = 1/\omega_P C_P \\ X_{LS} = \omega_P L_S \; X_{CS} = 1/\omega_P C_S \; X_{MP} = \omega_P M_P \; R_{\text{eq}} \\ \qquad = 8R_L\left(\pi^2\right)^{-1} \end{cases}. \tag{4}$$

Substituting (1), (2), and (4) into (3), U_L can be calculated as

$$U_L = \frac{M_P U_{\text{dc}}}{L_T}\sin\frac{\delta}{2}. \tag{5}$$

It is obvious from (5) that the output voltage U_L of the power transfer channel is irrelevant to the load. Instead, it is determined by U_{dc}, δ, L_T, and M_P.

C. Analysis of the Data Transfer Channel

As can be seen from Fig. 3, the processing circuit to implement the data transfer consists of an amplitude shift keying (ASK) modulation module achieved by CD4051 chip, a class-AB power amplifier achieved by 2N5551 and 2N5401, a bandpass filter by using ceramic filter, an envelope detector, an operational amplifier achieved by LT1816 chip, and a comparator by using LM311 chip. The generation of the ASK data carrier can be expressed as [4]

$$C\left(t\right) = \begin{cases} A_C\cos\left(2\pi f_D t\right), & \text{"0"} \\ 0, & \text{"1"} \end{cases} \tag{6}$$

where f_D and A_C are the operating frequency and the amplitude of the data carrier, respectively. $\dot{U}_{DP}$ is the output voltage of the power amplifier. $R_{D\text{eq}}$ is the equivalent input resistance of the bandpass filter [4]. By applying KVL in data transfer channel, the following equations can be obtained:

$$\begin{cases} \dot{U}_{DP} = jX_{LDP}\dot{I}_{DP} - jX_{MD}\dot{I}_{DS} \\ 0 = -jX_{MD}\dot{I}_{DP} + \left(jX_{LDS} + R_{D\text{eq}}\right)\dot{I}_{DS} \\ \dot{U}_{DS} = R_{D\text{eq}}\dot{I}_{DS} \end{cases} \tag{7}$$

where

$$\omega_D = 2\pi f_D \; X_{LDP} = \omega_D L_{DP} \; X_{LDS} = \omega_D L_{DS} \; X_{MD} = \omega_D M_D. \tag{8}$$

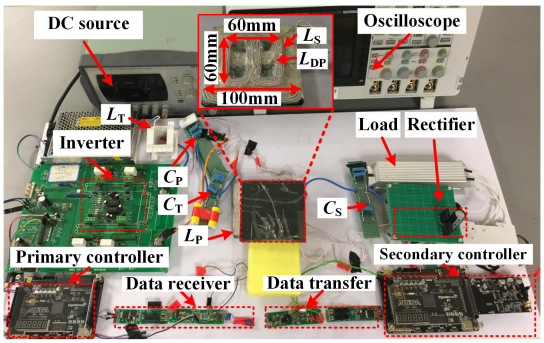

Fig. 4. Experimental setup.

Submitting (8) into (7), the input voltage $\dot{U}_{DS}$ of the bandpass filter can be obtained as

$$\dot{U}_{DS} = \frac{\dot{U}_{DP} R_{\mathrm{Deq}} M_D}{jL_{DP}L_{DS}\omega_D - j\omega_D M_D^2 + L_{DP}R_{\mathrm{Deq}}}. \quad (9)$$

By taking the derivative of the amplitude of $\dot{U}_{DS}$ with respect to M_D, one can obtain

$$\frac{d\left|\dot{U}_{DS}\right|}{dM_D} = \frac{\left(\frac{1}{k_{DPDS}^4} - 1\right)\omega_D^2 M_D^4 + L_{DP}^2 R_{\mathrm{Deq}}^2}{\sqrt{\left[\left(\frac{1}{k_{DPDS}^2} - 1\right)^2 \omega_D^2 M_D^4 + L_{DP}^2 R_{\mathrm{Deq}}^2\right]^3 \Big/ \left|\dot{U}_{DP}\right|^2 R_{\mathrm{Deq}}^2}}. \quad (10)$$

As can be seen from (10), since the coupling coefficient k_{DPDS} between L_{DP} and L_{DS} is smaller than 1, the amplitude of $\dot{U}_{DS}$ increases with M_D, and so does data transfer capability [4], [12].

D. System Control

The control diagram of the proposed system is shown in Fig. 3 with the conduction angle δ as the control variable. There are two controllers, i.e., primary controller and secondary controller. Secondary controller samples the output voltage U_L by using ADC module after the voltage divider, and then injects this information into the data transfer channel. With the proposed data transfer method, this information can be transferred from the secondary side to the primary side wirelessly. The primary controller picks up the information of U_L after the data demodulation. The error between the feedback voltage U_L and the reference $U_{L\mathrm{ref}}$ is sent to the proportional–integral controller for conduction angle δ calculation. Finally, the PSM controller generates the gate driving signals to control the inverter.

IV. Experimental Verifications

A laboratory prototype is built, as shown in Fig. 4. Data transfer rate is 19.2 kb/s. MOSFET IRF540 is used to construct the inverter. The utilized oscilloscope is MDO3024 from Tektronix. The values of the mutual inductances and self-inductances are measured by Agilent E4980A LCR. The parameters of the system are listed in Table I.

TABLE I
System Parameters

U_{dc}	L_P	L_S	L_T	C_P	C_S	R_{Deq}
50V	24.07μH	23.88μH	8.59μH	40.93nF	26.52nF	470Ω
C_T	L_{DP}	L_{DS}	$U_{L\mathrm{ref}}$	f_P	f_D	
73.66nF	10.87μH	10.96μH	35V	200kHz	6MHz	

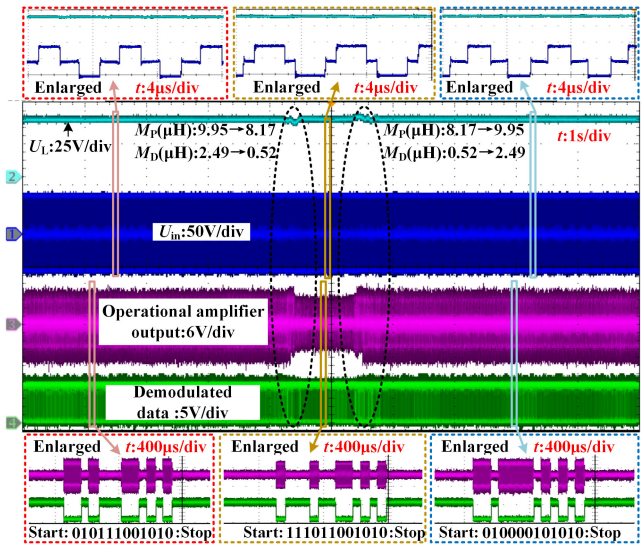

Fig. 5. Dynamic tracking process when the position of the secondary side is changed.

First, the misalignment ability of the system is tested. The position of the secondary side is changed from (0 mm, 0 mm) to (10 mm, −20 mm) and back to (0 mm, 0 mm). As a result, M_D varies from $M_{D\mathrm{MAX}}$ to $M_{D\mathrm{MIN}}$ and back to $M_{D\mathrm{MAX}}$, while M_P changes from $M_{P\mathrm{MAX}}$ to 8.17 μH and back to $M_{P\mathrm{MAX}}$. Load R_L is fixed at 10 Ω under misalignments. As shown in Fig. 5, it can be seen that U_L can be controlled to a steady state of 35 V regardless of M_P variation. From the enlarged view, it can be observed that the conduction angle δ of the inverter increases with the decrease of M_P. The output of the operational amplifier decreases with the decrease of M_D. But the data can still be demodulated. It is noted that the transferred data bits consist of a 12-b sampling value of U_L, together with a start bit "0" and a stop bit "1." The lower (left) bits of the sampled data may fluctuate within precision.

Fig. 6 shows the dynamic response when the reference voltage $U_{L\mathrm{ref}}$ is changed from 35 to 30 V and back to 35 V. It can be seen that the output voltage U_L tracks the reference tightly. It first decreases from 35 to 30 V with a fast transient of 90 ms, and then increases from 30 to 35 V with a response time of 130 ms. From the enlarged view, it can be seen that both the conduction angle δ and the sampled data are decreased accordingly with the decrease of $U_{L\mathrm{ref}}$.

Fig. 7 shows the dynamic response when the load R_L is changed from 10 to 20 Ω and back to 10 Ω. It can be seen that U_L can be maintained to a steady state of 35 V with a slight

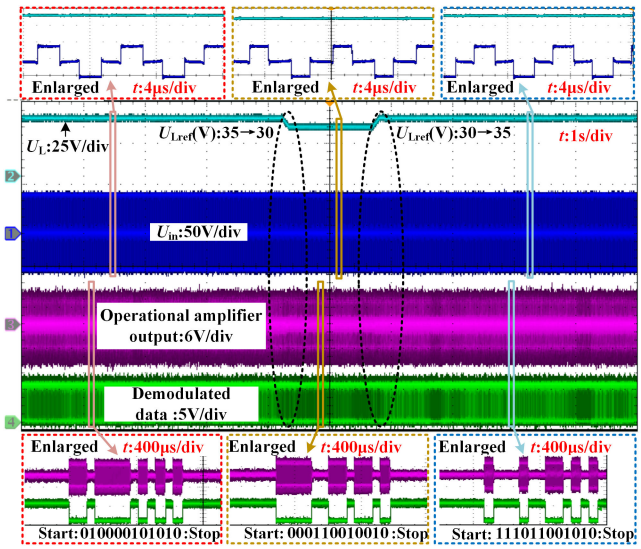

Fig. 6. Dynamic tracking process when U_{Lref} is changed.

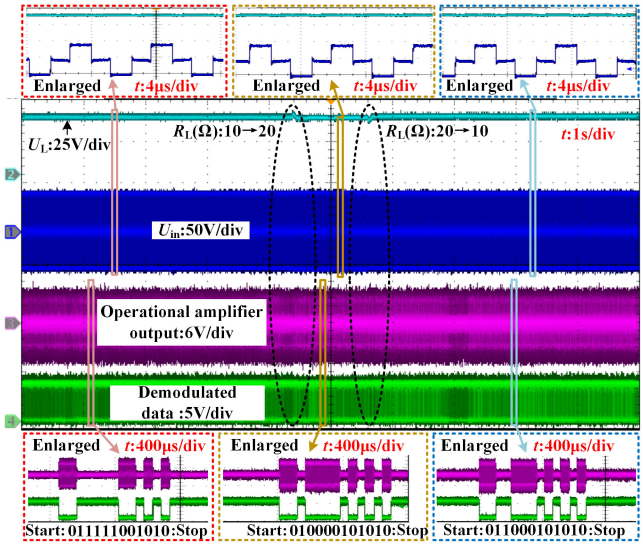

Fig. 7. Dynamic tracking process when R_L is changed.

overshoot. From the enlarged view, we can see that the conduction angle δ is constant regardless of the variation of R_L. Only the lower bits of the sampled data fluctuate slightly but it is acceptable since U_L is constant. When $R_L = 10\,\Omega$, the measured overall (dc–dc) power transfer efficiency is 87%.

V. Conclusion

A power and data-parallel transmission method based on a magnetically decoupled coupling structure is proposed. Unipolar coils are used for power transfer, while series-connected perpendicular bipolar coils are used for data transfer. Especially, the side lengths of data transfer coils are intentionally designed to be smaller than power transfer coils. Thus, in a specific four-quadrant misalignment area, the crosstalk interference between power and data transfer channels can almost be neglected. And the data transfer has the symmetrical misalignment ability within the specific misalignment area. An experimental prototype is built, and the output voltage is sent back to the primary side through the data transfer channel for closed-loop control. The experimental results show good consistency with the theoretical analysis. The proposed method can be used in wireless charging systems for EVs, robots, and mobile phones.

References

[1] L. Ji, L. Wang, C. Liao, and S. Li, "A simultaneous wireless power and bidirectional information transmission with a single-coil, dual-resonant structure," *IEEE Trans. Ind. Electron.*, vol. 66, no. 5, pp. 4013–4022, May 2019.

[2] C. C. Huang, C. L. Lin, and Y. K. Wu, "Simultaneous wireless power/data transfer for electric vehicle charging," *IEEE Trans. Ind. Electron.*, vol. 64, no. 1, pp. 682–690, Jan. 2017.

[3] J. Wu, C. Zhao, Z. Lin, J. Du, Y. Hu, and X. He, "Wireless power and data transfer via a common inductive link using frequency division multiplexing," *IEEE Trans. Ind. Electron.*, vol. 62, no. 12, pp. 7810–7820, Dec. 2015.

[4] X. Li, C. Tang, X. Dai, P. Deng, and Y. Su, "An inductive and capacitive combined parallel transmission of power and data for wireless power transfer systems," *IEEE Trans. Power Electron.*, vol. 33, no. 6, pp. 4980–4991, Jun. 2018.

[5] Z. Yan, Z. Xiang, L. Wu, and B. Wang, "Study of wireless power and information transmission technology based on triangular current waveform," *IEEE Trans. Power Electron.*, vol. 33, no. 2, pp. 1368–1377, Feb. 2018.

[6] Y. Son and B. Jang, "Simultaneous data and power transmission in resonant wireless power system," in *Proc. Asia-Pac. Microw. Conf.*, Jan. 2013, pp. 1003–1005.

[7] G. Wang, P. Wang, and Y. Tang, "Analysis of dual band power and data telemetry for biomedical implants," *IEEE Trans. Biomed. Circuits Syst.*, vol. 6, no. 3, pp. 208–215, Jun. 2012.

[8] Y. Sun, P. X. Yan, Z. H. Wang, and Y. Y. Luan, "The parallel transmission of power and data with the shared channel for an inductive power transfer system," *IEEE Trans. Power Electron.*, vol. 31, no. 8, pp. 5495–5502, Aug. 2016.

[9] A. Zaheer, H. Hao, G. A. Covic, and D. Kacprzak, "Investigation of multiple decoupled coil primary pad topologies in lumped IPT systems for interoperable electric vehicle charging," *IEEE Trans. Power Electron.*, vol. 30, no. 4, pp. 1937–1955, Apr. 2015.

[10] Y. Li *et al.*, "Reconfigurable intermediate resonant circuit based WPT system with load-independent constant output current and voltage for charging battery," *IEEE Trans. Power Electron.*, vol. 34, no. 3, pp. 1988–1992, Mar. 2019.

[11] Y. Li *et al.*, "A new coil structure and its optimization design with constant output voltage and constant output current for electric vehicle dynamic wireless charging," *IEEE Trans. Ind. Inform.*, to be published, doi: 10.1109/TII.2019.2896358.

[12] Z. Qian, R. Yan, J. Wu, and X. He, "Full-duplex high-speed simultaneous communication technology for wireless EV charging," *IEEE Trans. Power Electron.*, to be published, doi: 10.1109/TPEL.2019.2909303.